Carcinogen induced expansion of atypical B cells and pre-treatment tumor adjacent tertiary lymphoid structures associate with poor response to BCG in non-muscle invasive bladder cancer

Priyanka Yolmo, Sadaf Rahimi, Stephen Chenard, Gwenaelle Conseil, Danielle Jenkins, Kartik Sachdeva, Isaac Emon, Jake Hamilton, Minqi Xu, Manu Rangachari, David M. Berman, D. Robert Siemens, Madhuri Koti*

Graphical Abstract

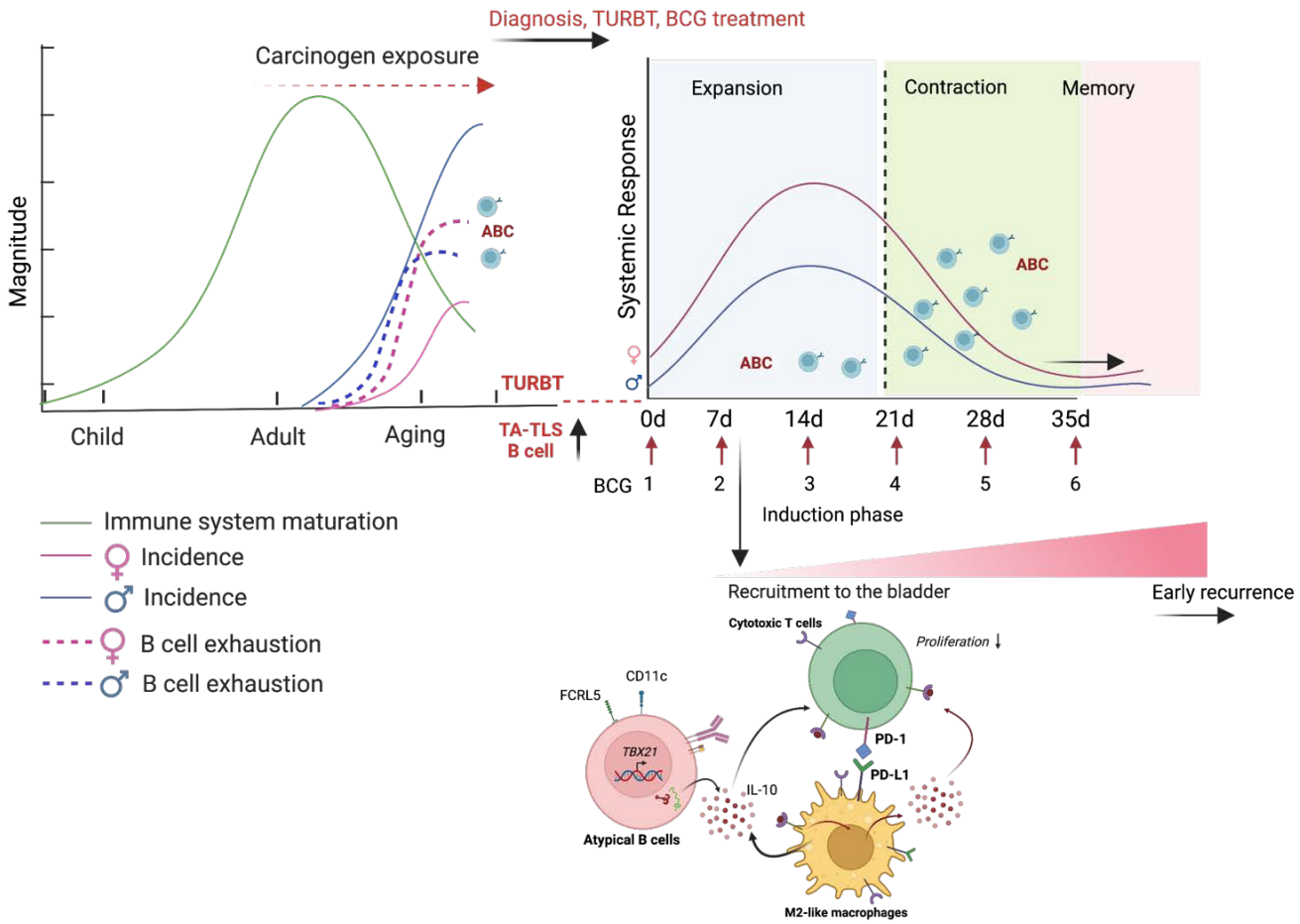

*Correspondence
kotim@queensu.ca

Carcinogen induced expansion of atypical B cells and pre-treatment tumor adjacent tertiary lymphoid structures associate with poor response to BCG in non-muscle invasive bladder cancer

Priyanka Yolmo‡[1,2], Sadaf Rahimi‡[1,2], Stephen Chenard[1,2], Gwenaelle Conséil[1,2], Danielle Jenkins[3], Kartik Sachdeva[1,2], Isaac Emon[1,2], Jake Hamilton[1], Minqi Xu[3], Manu Rangachari[4] David M. Berman[2,3], D. Robert Siemens[1,2,5], Madhuri Koti*[1,2]

[1]Department of Biomedical and Molecular Sciences, Queen's University, Kingston, ON, Canada; [2]Cancer Research Institute, Queen's University, Kingston, ON, Canada; [3]Pathology and Molecular Medicine, Queen's University, Kingston, ON, Canada; [4]Department of Molecular Medicine, Faculty of Medicine, Université Laval, Quebec City, QC, Canada; [5]Department of Urology, Queen's University, Kingston, ON, Canada.

Key words: Atypical B cells, tertiary lymphoid structures, NMIBC, BCG immunotherapy, sex differences

‡Equal Contribution
*To whom correspondence should be addressed
e-mail: kotim@queensu.ca
Date: December 28, 2022

Abstract

Intravesical bacillus Calmette-Guérin (BCG) G immunotherapy is the gold standard treatment for patients with non-muscle invasive bladder cancer (NMIBC). Unfortunately, more than 50% patients experience early recurrence or progression. Increased intra-tumoral immune infiltration in pre-treatment tumors has been shown to associate with poor outcomes post BCG therapy. Specifically, we recently showed that high intra-tumoral B cell density was associated with early recurrence and progression of NMIBC. Here, we address a major knowledge gap in the role of BCG induced expansion of a B cell population called, 'atypical B cells (ABCs)' in the context of age and sex, the two major variables in the pathophysiology of NMIBC. We first investigated whether pre-BCG TLSs associate with response to BCG. Using multiplex immunofluorescence and NanoString GeoMx digital spatial profiling-based characterization, we found higher density of tumor adjacent (TA) TLSs in patients categorized as BCG non-responders. Spatial proteomic profiling of 49 immune function and phenotype associated proteins revealed increased expression of immune exhaustion associated proteins in pre-BCG TLSs in tumors from both BCG responders and non-responders.

It is established that patient age is a risk factor associated with poor outcomes in NMIBC and that biological aging associates with exhausted populations of immune cells. The expansion of ABCs is known to accompany biological aging and repetitive immunizations. We hypothesized that ABCs are recruited to the bladder mucosa due to repeated BCG instillations in the induction phase and dampen local anti-tumor immunity in patients deemed as BCG non-responders. Using the N-butyl-N-(4-hydroxybutyl) nitrosamine (BBN) carcinogen induced murine model, we investigated the role of B cells in BCG response in aging mice. Bladder local and systemic immune alterations were characterized at post BCG therapy with or without B cell depletion. Since B cells exhibit significant shifts with biological aging in a sex associated manner, we used the four-core genotype mouse model to determine such differences following repeated treatment with BCG. BCG treatment in combination with B-cell depletion led to distinct bladder immune microenvironment states and systemic immune profiles.

Overall, this study demonstrates the significant role of ABCs in disease progression and that the B cell infiltrated pre-BCG therapy TA-TLSs reflect a systemically exhausted B cell functional state in patients deemed as BCG non-responders. Findings from this study provide the first evidence suggesting the role of B cells/ABCs in BCG response and will inform future translation to development of therapies along the B cell exhaustion axis.

1. Introduction

Bladder cancer (BC) is the most common urological malignancy known worldwide with 573,278 cases being diagnosed in 2020.[1] BC is more common in men as it is in women [4:1 ratio].[2] The majority of BC patients (75-85%) are diagnosed with early-stage NMIBC. Despite the lower incidence, women generally present with advanced stage tumors and experience shorter progression free survival.[3-6] Following trans-urethral resection of bladder tumor (TURBT), patients

categorized as intermediate or high-risk NMIBC are treated with intravesical bacillus Calmette-Guérin (BCG) immunotherapy.[7] The treatment regimen involves an induction phase of 6 weekly instillations after tumor resection, followed by a maintenance schedule of 3 weekly instillations every 3-6 months for over 1-3 years depending on risk stratification.[8] Despite its proven efficacy, recurrence post BCG treatment occurs in over 50% of patients, requiring repeated treatments, continuous surveillance, and bladder removal surgery upon progression (observed in ~30% patients) to muscle invasive stage.[9,10] While some of the newer second line treatments have demonstrated modest benefits, these approaches do not increase primary response to BCG and are not indicated in the BCG naïve setting.[11,12]

The previous report by our group, investigating immune cell infiltration profiles in pre-treatment tumor specimens from two large independent (Kingston Health Sciences Center; KHSC and UROMOL) cohorts of patients with NMIBC, revealed significantly increased density of B cells in high grade tumors from patients who exhibited early recurrence irrespective of the treatment type.[13] Patients who recurred within 1 year of their TURBT also exhibited high stromal B cell density that significantly correlated with stromal M2-like macrophages. Several other reports have demonstrated the role of M2-like suppressive macrophages and exhausted populations of T cells within the NMIBC TIME,[14-16] however, the B cell mediated humoral responses (key to mucosal immunity)[17] remain poorly defined in the context of response to BCG and disease progression.

Tumor infiltrating B cells are mainly localized within stromal aggregates of immune cells called tertiary lymphoid structures (TLSs).[18] TLS formation in the bladder mucosa is induced due to chronic inflammation,[19] such as persistent urinary tract infection[20,21]; exposure to carcinogens such as smoking; immunomodulatory therapy[18]; or age-related increased systemic levels of tumor necrosis factor-α (TNF-α).[22,23] Indeed, our previous report established an increase in TLS density and maturation with advanced stages of bladder cancer.[24]

The average age of diagnosis for BC is ~73 years. Biological aging is accompanied by a decline in lymphopoiesis and depletion of naïve B cells from peripheral pools, with a simultaneous expansion of subpopulations such as atypical B cells (ABCs; also known as age-associated B cells).[25,26] Simultaneous to these processes, B cell proportions significantly increase at mucosal sites, predominantly within mucosa associated TLSs.[22,27-29] Repeated vaccination and chronic inflammation also lead to the expansion of circulating ABCs. Importantly, ABCs are: 1) observed at a significantly higher frequency in females compared to males;[26,30] 2) exhibit features of high self-reactivity; equipped with specialized antigen presenting ability; and 3) have a distinct transcriptional profile.[31-33] In addition, ABCs are known to produce high levels of IL-6 and TNF-α and may therefore, augment the suppression of B cell lymphopoiesis.[34-36] In aging mice, ABCs increase in the bone marrow with a more pronounced expansion in the spleen, produce autoantibodies and respond uniquely to innate/microbial stimuli.[32,37] A key feature of ABCs is their proliferative response to stimuli that activate endosomal nucleic acid sensing pathways (toll like receptors; TLR7/9) leading to production of immunosuppressive cytokines such as IL-10.[32,38-41]

BCG immunotherapy is known to activate both the innate and adaptive immune responses.[42,43] Following intravesical instillation, BCG bacteria are internalized by residual cancer cells, normal urothelial cells, myeloid and lymphoid cells located within the bladder mucosa.[44,45] BCG antigens activate various cytosolic and cell surface receptors, including TLR2/9 in professional antigen presenting cells (APCs), which leads to the production of immune cell recruiting chemokines.[46] While the literature to date provides an understanding of the mechanism of action of BCG, its mode of action and associated cascade of immune responses, following intravesical administration in patients with NMIBC, is still not completely understood. Furthermore, among the professional APCs mediating response to BCG, B cells, which are critical to mucosal immune response remain under-examined.

Based on our previous findings from pre-treatment patient tumor specimens, we hypothesized that BCG

induces the expansion of B cells/ABCs following repeated intravesical administration and thus play a significant role in mediating poor outcomes. In this study, we first characterized TLSs in pre-treatment tumors from patients categorized as BCG responders and non-responders using multiplex immunofluorescence (IF) and NanoString GeoMx digital spatial technology (DSP). Since B cells/ABCs exhibit a sex and age dependent expansion and response, we further investigated whether mucosal inflammation associated (chronic carcinogen or repeated BCG induced) expansion of B cells is dependent on age and sex via conducting studies in aging wild type C57BL/6 and four core genotype (FCG) mouse models. Findings from this study clearly demonstrate a central role of BCG-induced expansion of ABCs as one of the mechanisms underlying poor outcomes following BCG immunotherapy in NMIBC.

2. RESULTS

2.1 2 Pre-treatment tumor adjacent TLSs are higher in BCG non-responders

TLS formation is a hallmark of chronic inflammation at mucosal sites. Based on our previous observation on high stromal B cell density and its association with early recurrence and progression, we questioned whether pre-treatment TLSs associate with response to BCG. Histopathological evaluation of pre-BCG therapy whole tumor sections, from 28 patients with NMIBC (**Suppl. Table S1**), revealed the presence of both small and large immune cell aggregates within the lamina propria, indicating chronic inflammation in bladder mucosa (**Fig. 1A**). We observed a higher number of tumor adjacent (TA) TLSs in whole tumor sections from BCG non-responders compared to responders (**Fig. 1B**). To further determine the maturation stage of TLSs, we performed multiplex IF staining, which revealed varying organization and maturation stages of TLSs within the tumors from both BCG responders and non-responders (**Fig. 1C**).

2.2 Pre-BCG therapy TA-TLSs express high levels of immune exhaustion related proteins

Given the counterintuitive finding on the association of TA-TLSs with early recurrence, we further characterized the expression of 49 immune function related proteins (Suppl. **Table S2)** in a subset of 12 specimens (6 in each group of responders and non-responders) using NanoString GeoMx DSP technology **(Fig. S1)**. We did not find any significant differences in expression of proteins associated with immune regulatory functions between TLSs from responders and non-responders. When compared to the tumor epithelial compartment, TLSs from both responders and non-responders exhibited significantly higher expression of a) immune regulatory proteins such as CD25, ICOS, TIM3, VISTA, PD-L2, IDO-1; b) antigen presentation associated proteins such as B2M, CD11c, CD40; and c) immune cell phenotype associated proteins, CD45, CD20, CD3, CD4, CD56 and CD68 (**Fig. 1D, 1E, and 1F**). These findings suggest that TLSs represent chronic carcinogen induced inflammation in the bladder mucosa and harbor exhausted populations of immune cells at the time of TURBT.

2.3. Chronic exposure to BBN carcinogen leads to increased infiltration of B cells and ABCs in the bladder

To confirm the previously reported age/sex related shifts in B cell subsets, we first profiled B cells and ABCs in the spleen and bone marrow of 12-month-old (reflecting immune profiles of middle-aged humans[23]) C57BL/6 female and male mice. The total B220+CD19+ B cell population did not exhibit significant sex differences in both spleen and bone marrow (**Fig. 2A)**; however, splenic ABCs (CD21-/low CD11c+) were significantly higher in 12-month-old female mice compared to their male counterparts under healthy conditions (**Fig. 2A**). Moreover, the frequency of ABCs in the spleen was <u>10-fold</u> lower in young female mice compared to the aging female mice **(Fig S2B)**.

To determine whether BBN induced chronic inflammation in the bladder leads to increased recruitment of ABCs in the bladder microenvironment, we exposed 12-month-old female and male mice to BBN carcinogen for 12 weeks. To specifically determine cause and effect, we first assessed whether B cell depletion during BBN exposure attenuates the inflammation in bladder and delays cancer progression. Results from both local and systemic immune profiling assessments exhibited clear sex

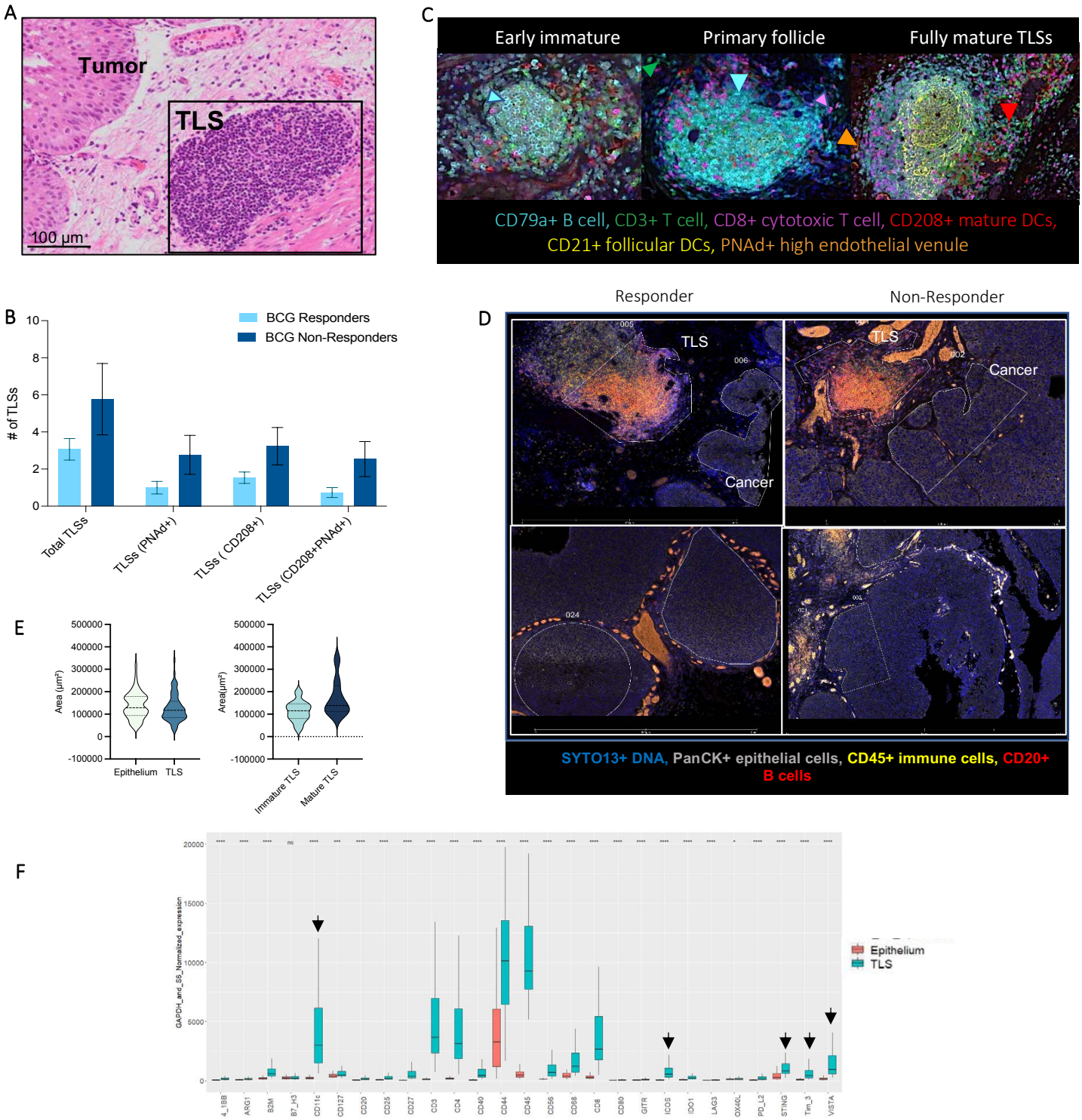

Figure 1. Pre-treatment tumors from BCG non-responders exhibit higher density of TA-TLSs. *H&E-stained whole tumor section from a patient classified as BCG non-responder (TLS highlighted in box)* ***(A);*** *Graph showing higher number of TA-TLSs in BCG non-responders (n=15) compared to responders (n=13) and distribution of different stages of TA-TLSs* ***(B)****. Multiplex IF showing different stages of TLSs in whole tumor sections* ***(C).*** *Representative images from NanoString GeoMx DSP based staining of 4 whole tumor sections (2 R and 2 NR), showing regions of interest (ROI) selection based on PanCK+, CD45+, CD20+ and SYTO 13+ areas/cells* ***(D).*** *Violin plot showing area distribution between TLSs and tumor epithelial compartments in all 12 sections* ***(E).*** *Box plots showing significantly differentially expressed proteins between tumor epithelial regions and TLSs* ***(F).***

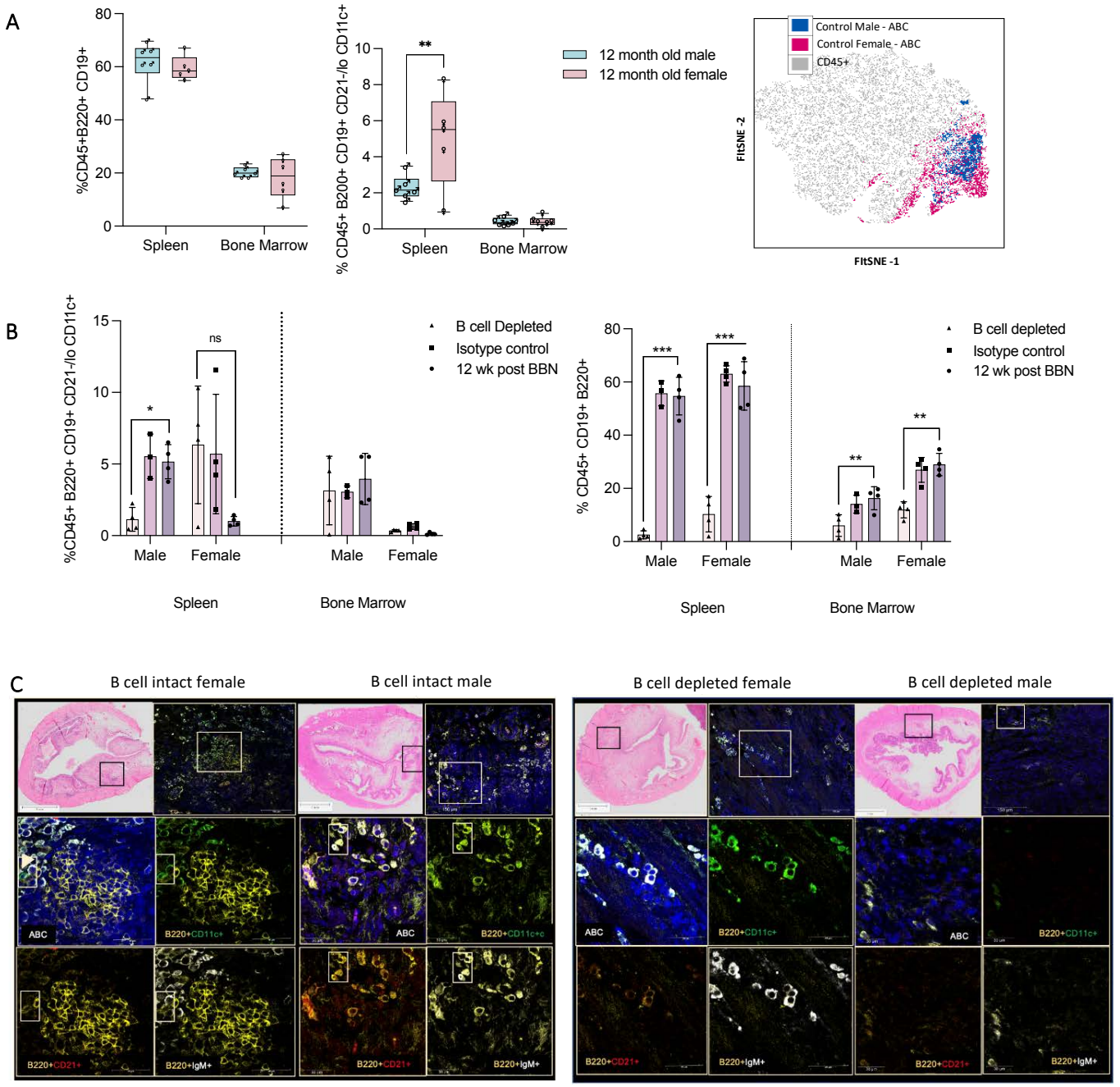

Figure 2. B cells and atypical B cells exhibit sex differences in aging C57BL/6 mice. *Comparison of total B cell (B220+ CD19+) and ABC (CD45+B220+CD19+CD21-/lo CD11c+) profiles in spleen and bone marrow of healthy 12-month-old female and male mice (**A**; n=4-6). Unsupervised Fast interpolation-based t-SNE (FItSNE) plot represents the distribution of ABC population in healthy 12-month-old female and male mice as a proportion of total CD45+ cells. FItSNE plot was created using FItSNE and FlowSOM tool in FlowJo® v10.81.1 software **(A).** Total B cells and ABCs in B cell depleted, isotype antibody injected and control female and male mice at 12 weeks post BBN initiation (**B**; n=3-4 mice/group). Analysis of flow cytometry data was performed using FlowJo® v10.81.1 software. All statistical analysis was performed using GraphPad Prism (v9.3.1). Representative multiplex IF images (n=4/group in each sex) showing differences in bladder infiltrating ABCs at 12 weeks post BBN exposure, with or without B cell depletion, in female and male mice **(C).** Ordinary one-way ANOVA with Tukey's post-hoc test was applied to determine statistical significance in differences (*p<0.05, **p < 0.01, ***p <0.001, ns – not significant). Bar graphs represent mean ± SD.*

differences with female mice showing increased frequency of splenic ABCs despite depletion **(Fig. 2B)**, and higher density of ABCs in the bladder microenvironment compared to their male counterparts (**Fig. 2C**). Histopathological assessment of whole bladder sections from B cell-depleted and B cell intact mice, revealed a benign and/or close to normal histology of the bladder urothelium (**Suppl. Fig. S3**) in the B cell depleted female mice whereas reactive atypia/dysplasia was present in majority of male mice and female mice that were exposed to BBN and did not undergo any depletion. Importantly this effect was captured early in females (***at week 12 post BBN+B cell depletion***) in contrast to males. Multiplex IF based spatial immune profiling of the bladders collected 1 week post last maintenance CD20 injection (12 weeks post BBN initiation) for B cell depletion revealed significantly fewer numbers of total B cells and ABCs in the B cell depleted group in comparison to the B cell-intact mice (**Fig. 2C**). These findings revealed increased recruitment or differentiation of B cells associated with chronic mucosal inflammation in the bladder microenvironment.

2.4 BBN and BCG induced expansion of splenic ABCs and bladder associated TLS formation is age and sex dependent

It is known that the X chromosome harbors genes such as *CD40L, CXCR3, TLR7, IL9R, IL13RA1/2* and *BTK*, all of which are involved in B cell function and regulation.[47] Moreover, *TLR7* and *IL13RA* play key roles in the expansion of ABCs. Exposure to BBN led to formation of TLSs in the wild type C57BL/6 female mice, as per our previous report (**Fig. 3E**). Indeed, the urothelium returned to its benign morphological states following the 1st dose of BCG, (**Fig. 3F)** in contrast to the saline treated mice where urothelial dysplasia/CIS was still present at this time point (not shown). However, at 1-6- and 8-weeks post completion of all 3 BCG doses, in both saline and BCG treated groups, urothelial dysplasia and progressive focal to widespread CIS and invasive carcinoma-like changes or papillary tumors were observed (**Fig. 3G-I**). Further, repeated BCG treatments also led to the formation of TLSs, as confirmed by IF staining in contrast to the bladders from saline treated mice where tumor growth with no TLS formation was observed, (**Fig. 3J and 3K**). An increase in splenic ABCs at 1 week post 1st BCG was observed compared to the pre-BCG levels (7-week post BBN exposure) in both the sexes, however, the magnitude was significantly higher in female mice (**Fig. 3B & 3C).** The frequency of ABCs post 1st BCG was similar to the age and sex matched healthy mice. A significant decline in post 3rd BCG proportions of splenic ABCs in both sexes indicated trafficking to bladder mucosa, which was also confirmed by histopathological evaluation and multiplex IF staining. These findings suggested that disease progression occurred during/post repeated BCG instillations simultaneous to treatment induced immune cell recruitment and potential exhaustion given the age and sex of mice.

We then addressed the fundamental question of whether sex associated ABC expansion in BBN exposed and BCG treated mice is influenced by gonadal hormones or sex chromosome complement or a combination of both factors. We used 12-month-old FCG mouse model to investigate these interactions (**Fig. 4A**). While no significant differences in the total CD19+ B cells were observed between the four genotypes (XXF (female gonads), XYF (female gonads), XXM (male gonads) and XYM (male gonads) (**Fig. 4B**) of the FCG mice, XXF mice exhibited significantly higher ABCs compared to all other genotypes (**Fig. 4C**). We then investigated the sex associated expansion of ABCs in BBN exposed BCG treated FCG mice. Splenic ABCs significantly increased post 3rd BCG dose in the XXF mice compared to the BBN exposed untreated group at the same time point (**Fig. 4C**). Such significant shifts were not observed in any other genotype of the FCG mice indicating that ABC expansion is a plausible effect of X chromosome associated and hormonal factors. Histopathological evaluation revealed the presence of higher density of lymphoid aggregates in the bladder lamina propria of XXF mice at this time point compared to XYF mice. Similarly, H&E staining revealed an overall higher immune cell infiltration in the XXM mice compared to the XYM mice (**Fig 4D**). These findings indicate a sex and age associated role of ABCs in mediating response to BCG.

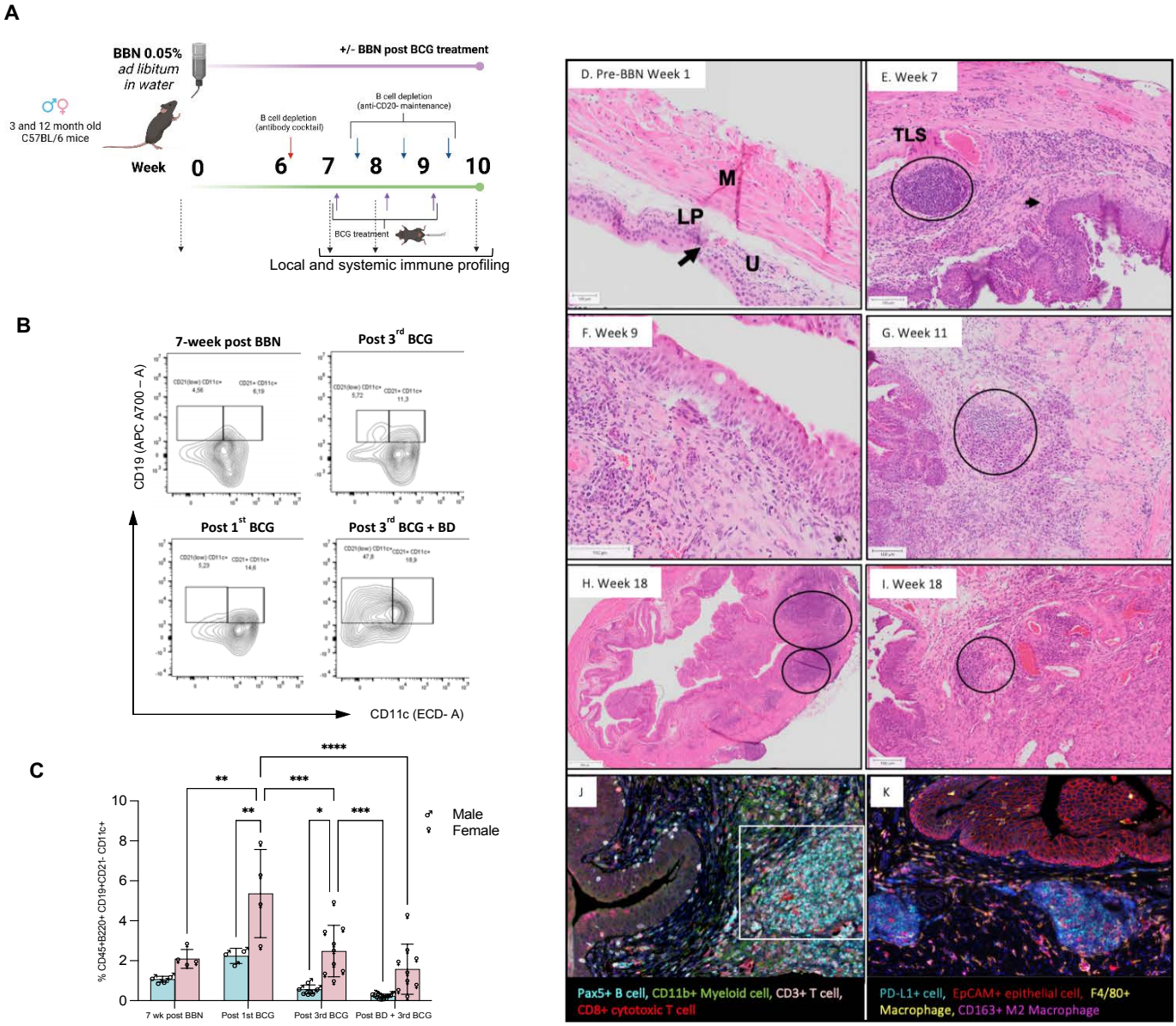

Figure 3. Repeated exposure to BCG in aging mice promotes expansion of ABCs and disease progression. *Schematic diagram showing experimental approach for intravesical BCG treatment (3 weekly doses) with or without B cell depletion (BD) in 12-month-old female and male mice* ***(A).*** *Representative contour plots for identification of splenic ABC population at different time points post BBN and BCG treatment. Contour plots are illustrative of frequency of CD19+ cells and may show disparity in density in comparison to bar graph as shown in B cell depleted and post 3rd BCG treatment group* ***(B).*** *Bar graph showing the frequency of ABCs (CD19+ CD21-/low CD11c+) post BBN and BCG treatment at different time points for both male (n=3-9) and female mice (n=4-9;* ***C****). H&E-stained sections showing histological changes in the urothelium and bladder microenvironment at various time points; pre-BBN* ***(D),*** *post 7-week BBN* ***(E)*** *post 1st BCG* ***(F),*** *post 3rd BCG* ***(G)*** *and 8-week post 3rd BCG* ***(H&I).*** *Bar graph represents mean ± SD. GraphPad software (version 9.3.1) was used to determine statistically significant differences in profiles across the different genotypes using two-way ANOVA with Tukey's multiple comparison test (*p<0.05, **p<0.001, ****p<0.0001, ns – not significant). Multiplex IF stained bladder sections showing TLS and immune cell infiltration post 3rd BCG instillation (****J and K****; 200x magnification). Circles indicate lymphoid aggregates/TLSs. L= Lamina propria, M: Muscularis propria, U= Urothelium. Scale bar in H&E-stained images– 100 µm.*

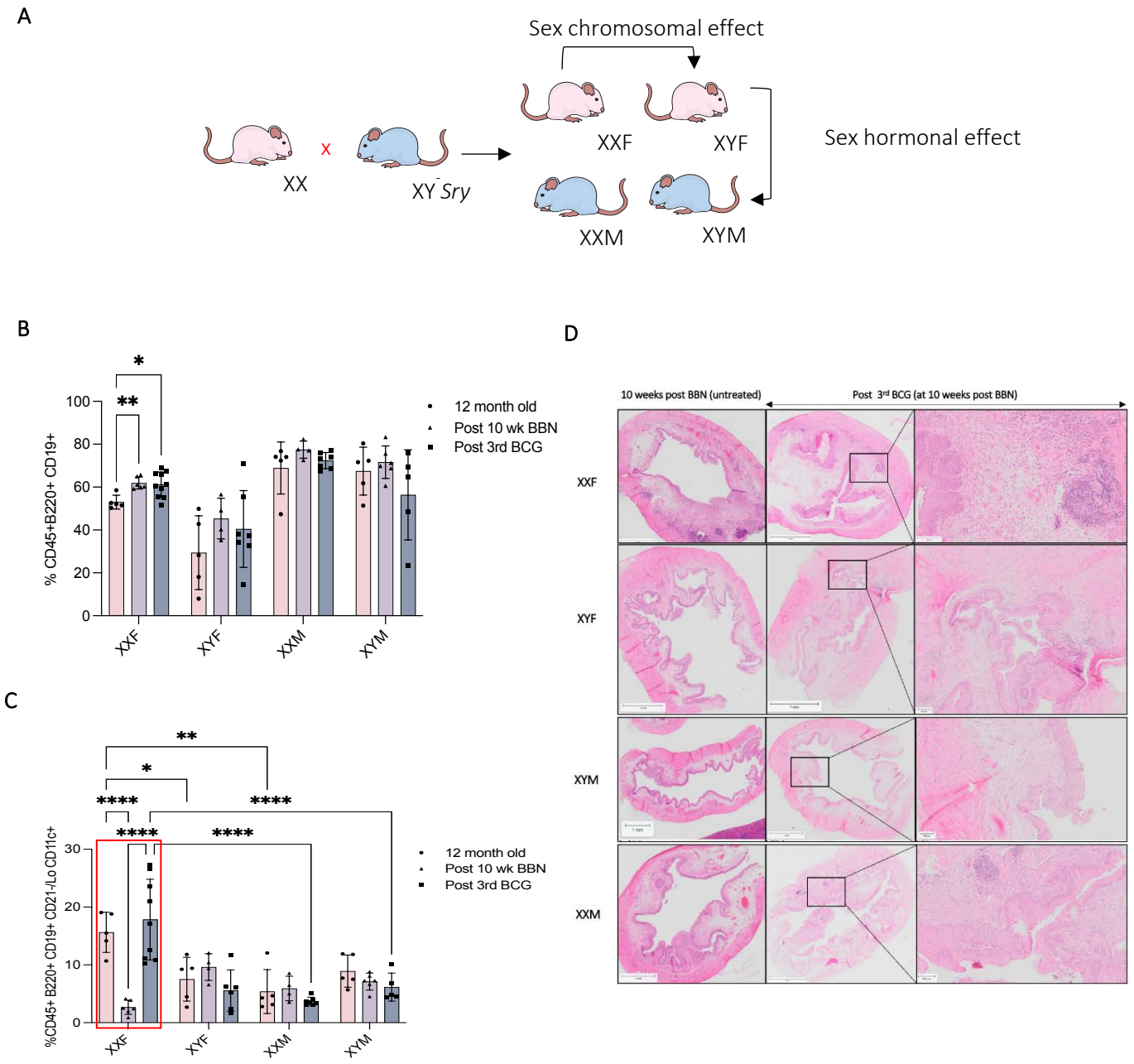

Figure 4. Expansion of ABCs is influenced by hormonal and sex chromosome associated factors. *Schematic representation of four core genotype (FCG) mouse model used to study the hormonal and chromosomal effect on BBN and BCG treatment induced ABCs* ***(A)****. Bar graph (mean ± SD) showing frequency of splenic B220+ CD19+ total B cells* ***(B)*** *and CD45+B220+CD19+CD21-/low CD11c+ ABC population determined using multiparametric flow cytometry* ***(C)*** *in healthy 12-month-old FCG mice; at 10-week post BBN and at 1 week post 3rd BCG instillation in BBN exposed mice (BCG treatment initiated at week 7 post BBN initiation). H&E-stained bladder sections from all four genotypes of FCG mice showing differences in bladder microenvironment and overall immune cell infiltration under untreated and BCG treated BBN exposed conditions* ***(D).*** *GraphPad software (version 9.3.1) was used to determine statistically significant differences in profiles across the different genotypes using two-way ANOVA with Tukey's multiple comparison test (*p<0.05, **p<0.001, ****p<0.0001, ns – not significant). N=4-9 per group.*

2.5. *In vivo* depletion of B cells during BCG treatment leads to enhanced recovery of the urothelium

We then asked the question whether B cell depletion alters response to BCG immunotherapy in mice with chronic exposure to BBN carcinogen. Depletion of B cells during BCG treatment led to the return of urothelium to its benign morphological state in female mice (**Fig. 5A**). In contrast, bladders from BCG treated B cell intact control female (**Fig. 5B** and male (**Fig. 5D)** mice showed dysplasia and focal CIS like changes at 1 week following completion of treatment with 3 doses of BCG). Reduced inflammation in the urothelium of female (**Fig. 5A**) and male mice (**Fig. 5C**) was observed in the B cell depleted groups albeit a more pronounced effect was evident in females. TLS formation was rare in the BCG + B-cell depleted mice (**Fig. 5E**) compared to B cell intact female mice (**Fig. 5F**). Exposure to BBN carcinogen was maintained throughout the course of BCG treatment and B cell depletion to mimic smoking behavior observed in patients during BCG treatment. Indeed, removal of the BBN carcinogen at the time of BCG treatment initiation in combination with B cell depletion revealed decreased invasion into the sub-mucosal region (data not shown). In mice undergoing BCG treatment and B cell depletion, the pattern of frequency of ABCs was similar to non-B cell depleted group potentially due to the baseline frequency of ABCs prior to BCG treatment initiation. These findings suggest that repeated weekly instillations of BCG lead to expansion and trafficking of ABCs to the bladder microenvironment. A combination effect of BBN carcinogen and BCG treatment induced sustained inflammation may cause systemic expansion of exhausted immune cells during the contraction phase thus augmenting disease progression.

2.6. B cell depletion during BCG treatment alters the frequencies of helper and cytotoxic T cell subsets

Given that BCG primarily activates the Th1 responses via activation of CD4 T helper cells, we explored the influence of B cell depletion on the profiles of T cell subsets and whether this occurs in a sex differential manner. We did not observe any significant sex differences in splenic total CD3+ T cell frequency at both early and late (post 3rd BCG) time points. However, in the bone marrow, the frequency of total CD3+ T cells was significantly higher in female mice post 3rd BCG in contrast to male mice (**Fig. 6A & 6B**). However, at this time point in the B cell depleted group there was a significant increase in total splenic T cell frequency compared to the B cell intact group in both sexes (**Fig. 6B**). Such a trend was not observed in the bone marrow profiles, where significant sex difference was observed in proportion of CD3+ T cells after repeated BCG treatment and B cell depletion. Splenic immune profiles of saline treated mice reflected catheterization induced sterile inflammation, an effect that has also been reported previously (data not shown). A BCG specific immune response was revealed by the changes in the urothelium and the T cell profiles in bone marrow where significantly increased CD3+ T cell proportions was seen only in female mice that received 3 doses of BCG with or without B cell depletion**.** A decline in splenic CD4+ T helper cells and CD8+ T cells following all 3 BCG instillations indicated potential recruitment to the bladder (**Fig. 6C - 6E**). Overall, these findings confirm that in response to administration of BCG via intravesical (mucosal) route, the host elicits BCG specific helper T cell associated response that augments a cancer cell specific cytotoxic immune response.

2.7. B cell depletion during BCG treatment of BBN exposed mice leads to elevated levels of plasma Th1 and Th2 proinflammatory cytokines in female mice

Multiplex cytokine profiling of plasma collected following completion of 3 doses of BCG treatment revealed significant differences in proinflammatory and immune cell activating cytokines key to mediating Th1 and Th2 responses. In female mice undergoing B cell depletion during BCG treatment, plasma levels of the Th1 cytokines; IL-2, IFN-γ, GM-CSF, MIP-1α and MIP-1β were significantly higher compared to mice that did not undergo B cell depletion during BCG treatment. Similarly, significantly increased Th2 cytokines such as IL-9 and IL-13 were observed in mice subjected to B cell depletion during BCG treatment (**Fig. 7**). These findings suggest a critical role of ABCs in inhibiting Th1 and Th2 responses induced by repeated mucosal BCG administration in female mice.

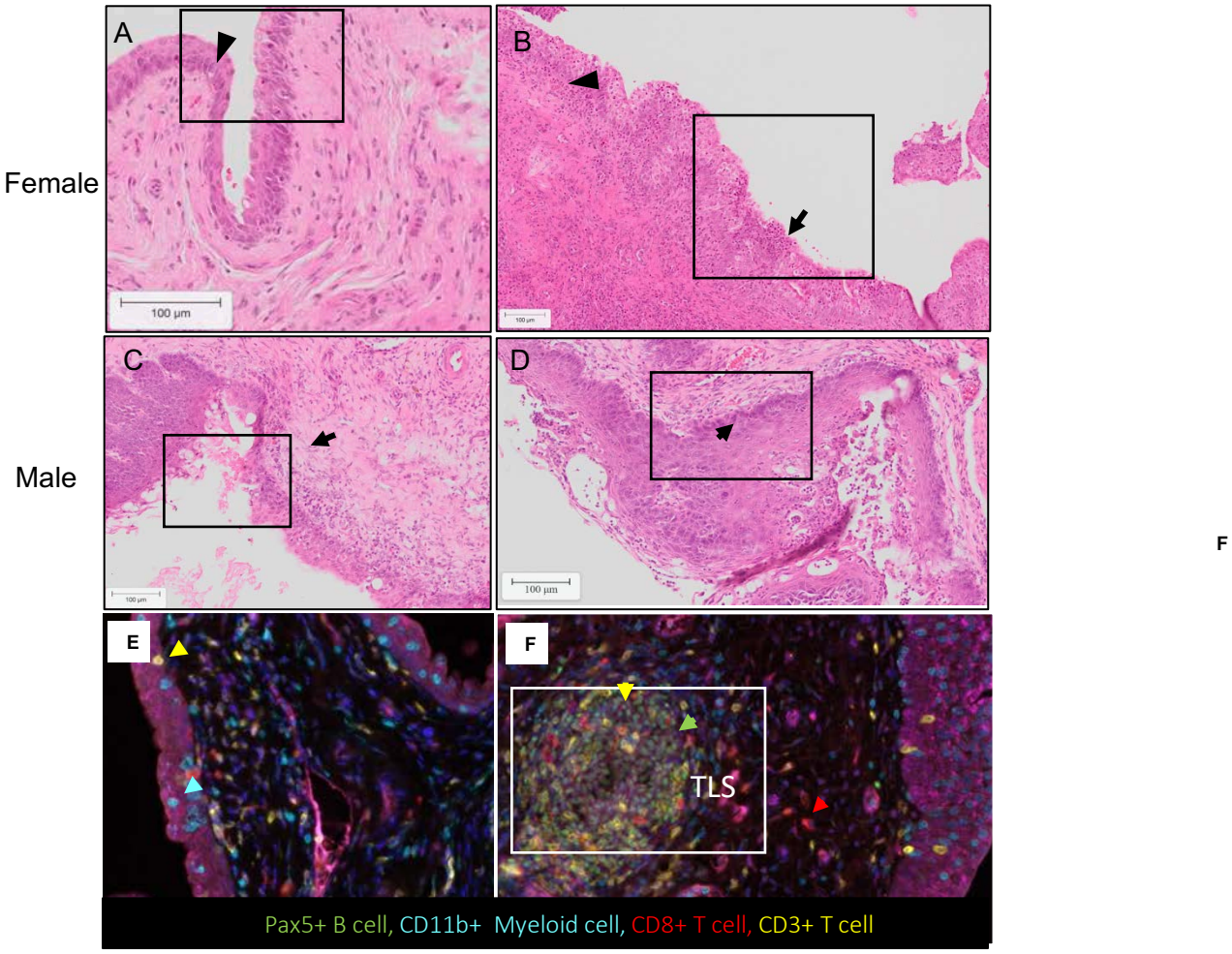

Figure. 5. Effect of transient B cell depletion during BCG treatment on urothelium of BBN exposed female and male mice. *H&E-stained whole bladder section showing benign/normal histology of urothelium post 3rd BCG + B cell depletion in female* ***(A)*** *and male* ***(C)*** *mice compared to dysplasia and CIS post 3rd BCG without B cell depletion in female* ***(B)*** *and male mice* ***(D).*** *Multiplex IF stained whole bladder section showing dysplasia and TLS formation (white box) post 3rd BCG instillation in BCG+ isotype treated mice (F) compared to in contrast to the BCG+ B cell depleted mice* ***(E).*** *Representative of 8-10 regions/section, 200x magnification (n=5/6 mice/group). Scale bar in H&E-stained images– 100 µm.*

2.8. B cell depletion during BCG treatment alters systemic and bladder infiltrating myeloid cell functional states

Bladder resident and recruited populations of myeloid cells are key to BCG response. BCG treatment led to significant alterations in the profiles of CD11b+ myeloid cells in spleen and bone marrow of both female and male mice. Overall female mice depicted a higher proportion of myeloid cells in the spleen compared to males. A significant increase in splenic CD11b+ cells, at 1 week post 1st BCG dose, was only observed in the female mice compared to the male mice (**Fig. 8A & 8B).** Following completion of treatment with all 3 doses of BCG, in both female and male mice, there was a significant decline in bone marrow CD11b+ cells in contrast to mice undergoing B cell depletion during BCG indicating potential trafficking to the bladder (**Fig. 8B**). This was also confirmed by spatial immune profiling of bladders from the same mice where increased density of macrophages were observed (**Fig. 8E & 8F).**

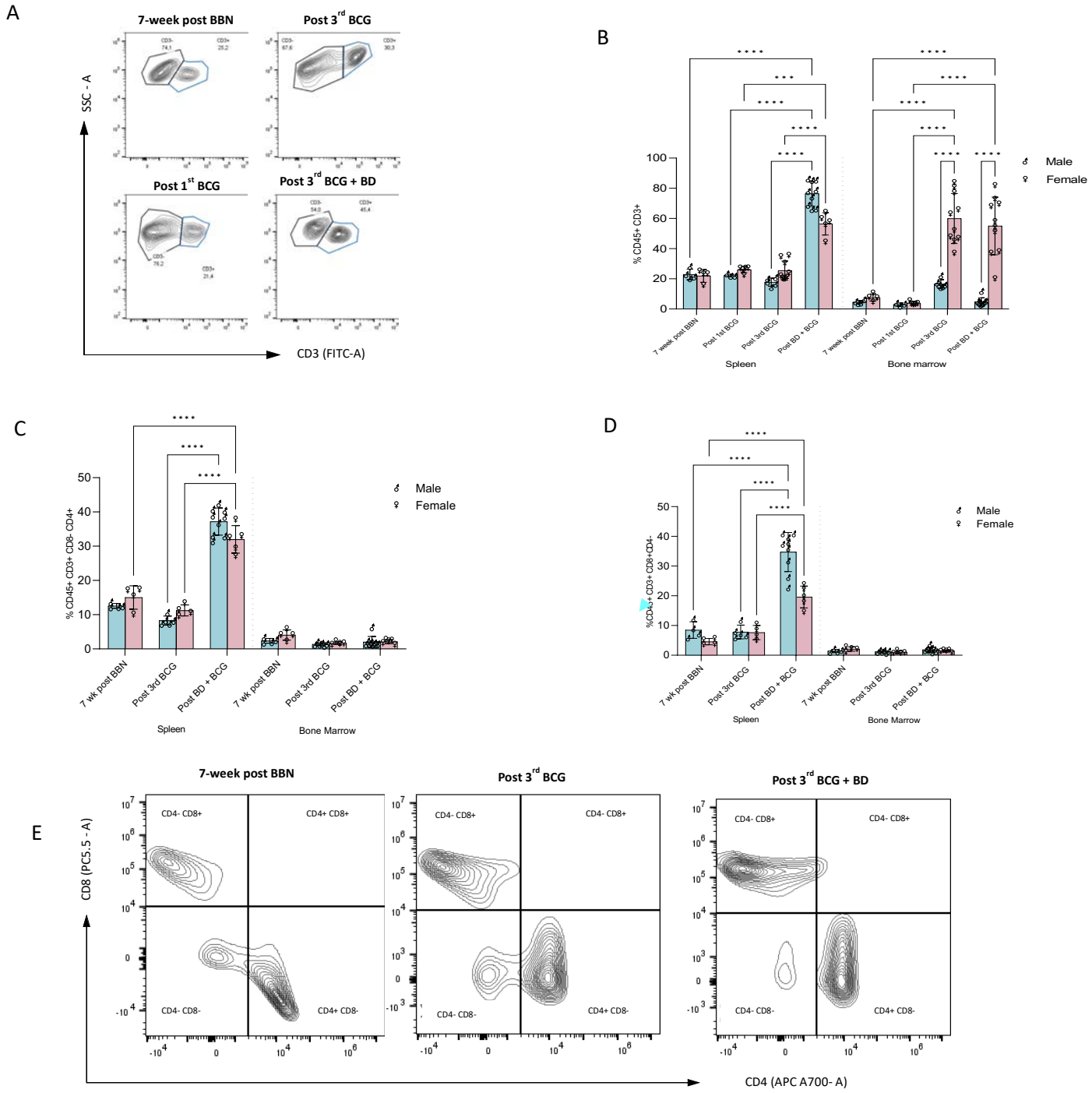

Figure 6. Depletion of B cells during BCG treatment alters systemic T cell profiles in BBN exposed female and male mice. *Representative flow cytometry contour plots demonstrating differences in splenic CD45+ CD3+ total T cell population in different treatment groups* ***(A)****. Bar graph showing frequency of total CD3+ T cells in the spleen and bone marrow of 12-month-old female and male C57BL/6 mice undergoing different treatments with or without B cell depletion (BD) as indicated* ***(B)****. Bar graph showing frequencies of CD4+ CD8- T cells* ***(C)*** *and CD4-CD8+ cytotoxic T cells* ***(D)*** *in the spleen and bone marrow of 12-month-old aging female and male mice in different treatments as indicated. Representative flow cytometry contour plots demonstrating differences in CD4+ CD8- and CD4- CD8+ T cell subsets in different treatment groups* ***(E).*** *Bar graphs represent mean ± SD. Analysis of flow cytometry data was performed using FlowJo® v10.81.1 software. All statistical analysis done in GraphPad Prism software (v9.3.1) using two-way ANOVA with Tukey's post hoc test depicted statistical significance. (***p < 0.001, ****p < 0.0001).*

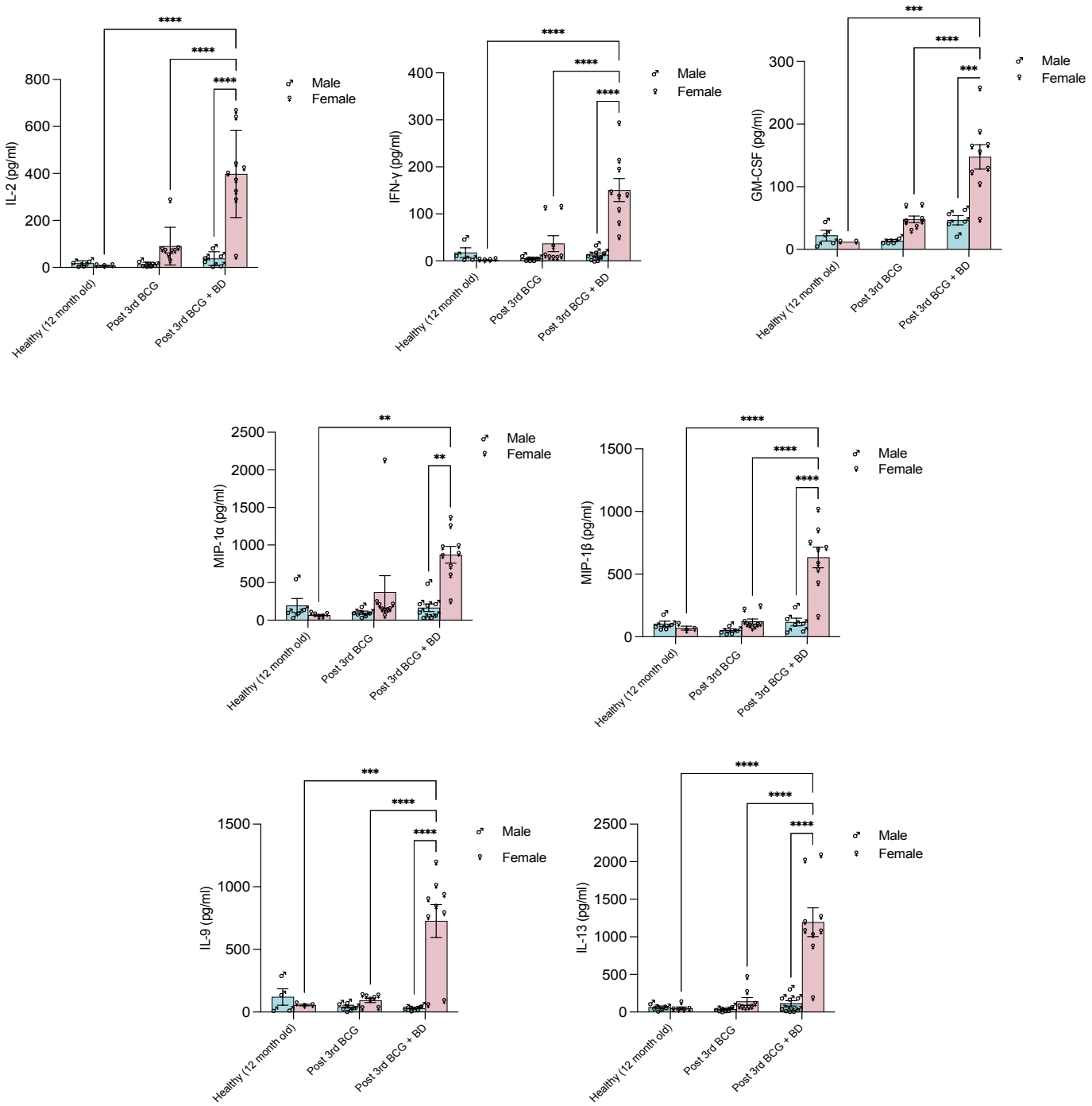

Figure 7. B cell depletion during BCG treatment increases plasma Th1/Th2 cytokine levels in female mice. *Plasma collected at 1 week post 3rd BCG dose with or without B cell depletion was subjected to multiplex cytokine profiling. Significantly increased levels of Th1 (IL-2, IFN-γ, MIP-1α, MIP-1β), Th2 (IL-9 and IL-13) cytokines and GM-CSF, were observed in BCG+B cell depleted (BD) female mice in contrast to male mice (n=3-4 in each group). Statistical significance, *p<0.01, **p<0.001, ***p<0.0001, ****p<0.0001, was determined using one-way ANOVA with Tukey's post-hoc test.*

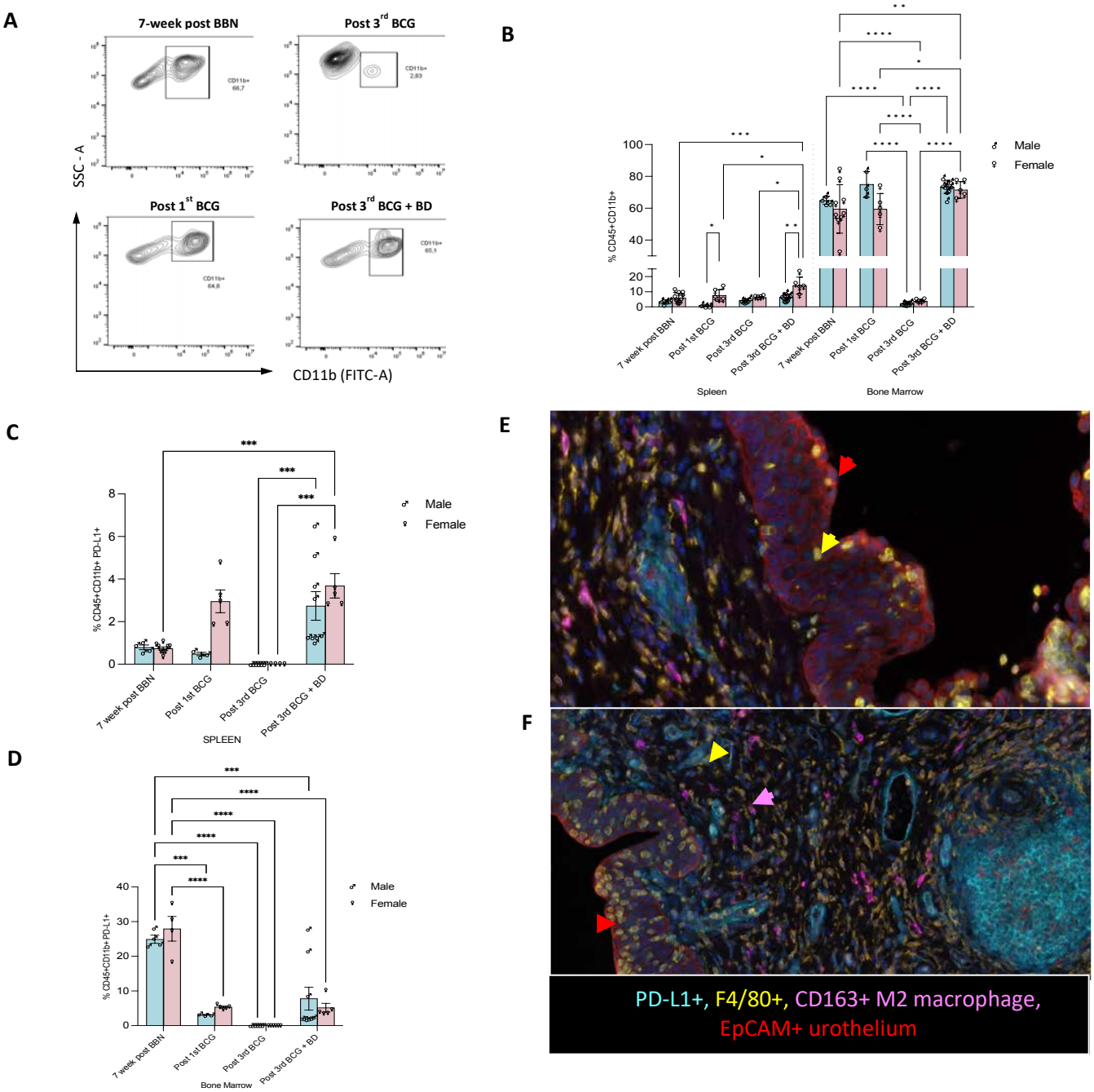

Figure 8. Repeated BCG treatment increases PD-L1 expression on splenic myeloid cells and in the bladder microenvironment. *Representative flow cytometry contour plots demonstrating differences in splenic CD45+ CD11b+ total myeloid cell population in different treatment groups* ***(A).*** *Bar graph showing frequencies of total CD11b+ myeloid cells in the spleen and bone marrow of 12-month-old female and male C57BL/6 mice undergoing different treatments as indicated* ***(B****). Bar graph showing differences in the profile of CD11b+ PD-L1+ cells in spleen* ***(C)*** *and bone marrow* ***(D)*** *of 12-month-old aging female and male mice in different treatment groups with or without B cell depletion (BD). Analysis of flow cytometry data was performed using FlowJo® v10.81.1 software. All statistical analyses were performed in GraphPad Prism software (v9.3.1) using two-way ANOVA with Tukey's post hoc test (*p<0.05, **p<0.001, ***p < 0.001, ****p < 0.0001). Bar graphs represent mean ± SD. Multiplex IF-stained whole bladder sections showing PD-L1+ cells in BCG + B cell depleted* ***(E)*** *and BCG + isotype antibody treated female mice* ***(F)*** *at 1 week post 3rd BCG instillation. Representative of 8-10 regions per section (n= 5/6 mice in each group). Images at 200X magnification.*

We then assessed the expression of PD-L1 immune checkpoint on myeloid cells. A significant increase in splenic PD-L1 immune checkpoint expressing myeloid cells was observed only in female mice following the 1st BCG dose (**Fig. 8C**). The proportion of PD-L1 expressing myeloid cells was significantly higher following the 3rd BCG dose in the spleen and bone marrow of both female and male mice that underwent in B cell depletion during BCG treatment. This was not the case for mice that did not undergo B cell depletion during BCG treatment (**Fig. 8C**). Multiplex IF based spatial immune profiling revealed that the BCG + isotype treated mice had increased infiltration of PD-L1+ cells in the urothelium and within and outside of TLSs compared to B cell depleted group (**Fig. 8E & 8F**). These findings indicate BBN and repeated weekly BCG induced sustained local inflammation may expedite the exhaustion of systemic and bladder local APCs.

3.0 Discussion

Patient age is an independent risk factor associated with poor response to BCG immunotherapy in NMIBC.[48] To date there has been a significant focus on investigating the spectrum of pre-treatment TIME and associated cancer cell intrinsic genetic alterations. Factors underlying the influence of age associated immune function decline on variable clinical outcomes following BCG immunotherapy in patients with NMIBC, have not been well studied. Bladder mucosa is constantly exposed to bacteria and toxins and thus the defense mechanisms at this barrier exhibit similarities with other mucosal surfaces such as the respiratory tract and the gut. These resemblances include the compartmentalization of T and B cells, and the presence of other APCs such as macrophages and follicular dendritic cells within TLSs. TLSs rely on a highly organized vascular system of high-endothelial vessels and often act as inductive sites for antigen uptake and *in situ* immune cell differentiation.[49]

Both B cells and TLSs have been shown to associate with favorable prognosis and response to chemotherapy or immune checkpoint inhibitor therapy in some cancers including muscle invasive BC (MIBC).[50-52] Recent reports also show that increased density and proximity of TA-TLSs were associated with improved survival in patients with MIBC who are treated with adjuvant chemotherapy.[53] Furthermore, the presence of TA-TLSs has been correlated with improved response in patients with MIBC treated with immune checkpoint inhibitors.[54] TA-TLSs are also associated with favorable prognosis for patients with melanoma, renal, gastric, and lung cancers.[55,56] Contrary to this, in colorectal, breast and hepatocellular carcinoma[57], a negative relationship between TA-TLSs and patient outcomes has been demonstrated.[58,59]

Similar to these, our previously reported findings based on pre-treatment tumors from patients with NMIBC are suggestive of their negative association with response to BCG.[13] This may primarily be attributed to the difference in local immunomodulation and downstream responses induced by live BCG bacteria compared to systemically administered immune checkpoint inhibitors or cytotoxic chemotherapy. The discrepancy also highlights the fact that the relationship between TA-TLSs and cancer patient outcome depends on several parameters, including functional states of immune cells within TLSs, cancer type/site, etiology, age/sex and disease stage. Supporting this notion, spatial proteomic profiling using the NanoString GeoMx DSP, allowed us to interrogate and confirm the abundance of immune activation and exhaustion related proteins within TLSs. While we observed high expression of immune cell exhaustion markers in pre-BCG TA-TLSs, it is plausible to suspect that the induction of TLSs post BCG would be associated with positive clinical outcomes given the ability of BCG to induce the formation of granulomas.[60] However, depending on the recruitment of exhausted immune cell populations such as ABCs from the systemic circulation following repeated exposure to BCG (as observed in our *in vivo* studies), this association may be reverse.

TLSs may thus play a pathological role by promoting auto-antibody production and harboring immunosuppressive and dysfunctional immune cell populations due to sustained local inflammation.[61] Indeed, previous reports in NMIBC showed significantly increased levels of circulating IgG antibodies in patients exhibiting early recurrence post BCG.[62] This duality helps to explain our findings as to why TLSs have been strongly associated with both positive and negative outcomes in different cancer types. In this study,

multiplex IF based characterization of TLSs did not reveal any significant differences in the density of TLSs in tumors from patients who subsequently responded, compared to those who exhibited early recurrence post BCG. However, the location and maturity of TLSs and proximity to tumor epithelial compartment was indicative of an aggressive tumor behavior and an exhausted local immune response. Nevertheless, our findings from a cohort of 28 patients (89% male patients) provide novel insights into TLS biology and emphasize the need for further validations in large independent cohorts. BCG immunotherapy in NMIBC is unique with respect to its mucosal route of administration and dosing schedule that requires repeated intravesical instillations at weekly intervals during both the induction and maintenance phases. Indeed, the age-related decline in humoral immunity and memory responses justifies the schedule of repeated administration in order to achieve the desired magnitude of anti-tumor immunity in majority of the patients. However, such repeated exposure to BCG antigens potentially also leads to expansion of exhausted immune cell populations in the effector memory phase, potentially following the 4th intravesical instillation. Such an expansion may occur specifically in BCG non-responsive patients with a history of chronic or persistent carcinogen exposure, smokers, patients with autoimmune conditions or female patients with a history of recurrent urinary tract infections. The recent report by Strandgaard and colleagues[15] demonstrated T cell exhaustion as a major factor underlying BCG failure. This finding supports a sustained '*inflationary T cell expansion*' phenomenon that has been described in the context of chronic lymphocyte choriomeningitis virus (LCMV) infections.[63]

Immunosenescence associated B cell alterations, governed by hormonal and sex chromosome associated factors, accompany aging in a sex differential manner.[25] Indeed, immune profiling of aging mice confirmed the higher frequency of ABCs in aging female mice compared to their male counterparts under physiological conditions. Most importantly, using the FCG mouse model, we clearly established that such sex differences in BCG induced systemic immune profiles as well as bladder associated lymphoid aggregate formation, are influenced by both hormonal and X chromosome linked factors. Indeed, the immune cell profiles post BCG treatment of wild type female and male mice further confirmed the age and sex associated expansion of systemic ABCs.

Based on our *in vivo* findings, we reason that BCG internalized by ABCs in the bladder microenvironment/TLSs, activates the TLR9 pathway following binding of bacterial CpG DNA.[40] Such an amplified TLR9 response could lead to the production of immunosuppressive IL-10, which may further inhibit anti-tumor T cell responses and polarize macrophages to M2-like suppressive states. Validation to the central role of B cells comes from the noteworthy observation that depletion of B cells during BCG treatment reduced inflammation in the urothelium and helped accelerate its recovery despite the presence of carcinogen in specifically in female mice. Recovery of urothelium was also accompanied by significant increases in circulating levels of the cytokines such as IL-2, IFN-γ, IL-9 and IL-13 that favor a Th1 and Th2 response. It is known that the cytokine IL-21 (inhibits CD8+ T cell cytolytic function), which governs ABC expansion plays opposite roles compared to those of IL-2 (promotes cytotoxic function of CD8+ T cells).[64] B cell depletion prior to initiation of BCG treatment may thus ablate such IL-21 mediated suppression of T cell function thus enhancing anti-tumor immunity especially in females or males with high TA-TLSs. We did not determine the source of these cytokines in our study, however, the significant increase in splenic CD4+ and CD8+ cells in B cell depleted male and female mice, is suggestive of their potential roles in secretion of these cytokines.

Our study is not without limitations. We did not establish the precise cellular trafficking associated events following BCG. However, our finding that CD3+CD8- T cells were significantly expanded post 3rd BCG in both B cell depleted and non-depleted mice, suggests that BCG bacteria travel to bone marrow where further cellular priming and activation may occur. While findings from this study demonstrate the critical role of B cells and ABCs in mediating response to BCG, the mechanistic basis of how these cells suppress anti-tumor cytotoxic response remains unclear and needs further investigation. Clearly, mouse models do not reflect the disease complexity observed in human scenarios. However, our study considers aging aspects of the immune system, unique aspects of

mucosal immune responses and investigation of sex differences via the use of FCG mice.

Overall, this study not only advances the current understanding of the BCG mode of action in the context of bladder mucosal immunity but also provides the first evidence for a critical role of B cell exhaustion, reflected by higher pre-BCG TA-TLSs and expansion of ABCs, in disease progression and treatment response. Another important and novel finding from our study is the sex differences in ABC expansion following BBN carcinogen exposure and BCG treatment. Taken together, these findings based on human specimens and *in vivo* studies partially explain the poor outcomes in female patients and in male patients with high intra-tumoral B cells and TA-TLSs in the pre-treatment tumors.

Conclusions and future perspectives

The treatment protocol for BCG immunotherapy in NMIBC involves repeated exposure at short intervals during the induction phase of treatment. It is plausible that in some patients, such repeated BCG induced immune activation will also lead to increase in exhausted memory B cells and their recruitment to the bladder microenvironment leading to less effective anti-tumor immune responses. This effect will be more pronounced in older patients or those who exhibit higher pre-BCG intra-tumoral density of B cells within TA-TLSs, reflective of their age-related/chronic carcinogen exposure induced profiles. Literature to date describes '*memory inflation*' as a feature of atypical T cells.[65-67] It is tempting to speculate that, analogous to this T-bet transcription factor associated fate in both T and B cells, expansion of ABCs (during the effector memory phase) may represent an '*inflationary B cell*' phenomenon that occurs due to repeated encounter with BCG bacteria and potentially amplified post 4th BCG instillation in the induction phase. This effect may potentially be more pronounced in female patients who generally experience poor outcomes. However, our previous report and unpublished findings suggest that male patients with high pre-treatment intra-tumoral B cell density also experience early recurrence post BCG, which indicates similar responses in both sexes. Our work in progress on systemic profiles of ABCs in patients undergoing BCG treatment supports this speculation (data not shown), however, awaits evaluation based on long term outcomes.

The current findings highlight that exhausted or dysfunctional states of immune cells within the pre-BCG TA-TLSs exist in tumors from BCG unresponsive patients. It is unclear whether these pre-treatment TLSs and tumor epithelial regions harbor tissue resident B cells that acquire a memory phenotype and differentiate in situ upon re-encounter with tumor antigen. Given the heterogeneity in tumor neoantigens, which is also influenced by the type of mutations acquired during post treatment progression, re-encounter of tumor specific antigens may not occur. In a classical germinal center reaction, resident memory B cells have been shown to proliferate and undergo selection within the draining lymph node. However, whether such prototypical reactions occur in the ectopic germinal centers such as TLSs is currently not clearly understood. Lastly, it is established that B cell associated CD21 (complement receptor 2) binds to autoantigens or immune complexes,[68] and also interacts with TLR9. Most importantly CD21/CR2 is critical for the internalization of BCG bacteria by B cells.[69] The role of complement cascade in mediating response to BCG in NMIBC has not been explored and needs further investigation.

Findings from our study provide a solid foundation for further investigations into B cell associated responses to BCG immunotherapy in NMIBC. Therapeutic targeting of ABC associated markers could be novel approach for treatment of patients identified early based on their systemic and bladder associated immune profiles.

4.0. MATERIALS AND METHODS

4.1 Human NMIBC tumor specimens

All studies involving the use of patient materials were approved by the Human Ethics Review Board at Queen's University. The cohort comprised of 28 patients (**25 males and 3 females**) with NMIBC who underwent TURBT surgery at KHSC between March 2016 and November 2017. Formalin-fixed paraffin-embedded (FFPE) tumor specimens were retrieved from the Department of Pathology at Queen's

University. Patient's clinical details were retrieved via electronic chart review. All patients in the cohort received adequate induction of BCG immunotherapy (>5 out of 6 doses) following index TURBT surgery. Response to BCG was defined as the time from each patient's earliest TURBT resection to next malignant diagnosis. Operative notes were reviewed to exclude re-resections as recurrences. Patients who had recurrence-free survival greater than 2 years were classified as BCG-responders (n=15). Patients who had recurrence-free survival less than 1 year were classified as BCG-non-responders (n=13).

4.2 Multiplex immunofluorescence on whole tumor sections

We employed multiplex IF to characterize the organization and maturity of TLSs found in tumors from NMIBC patients. Using our selected archival FFPE samples, triplicate 5 µm sections were cut and mounted at Queen's Laboratory for Molecular Pathology (QLMP). One section per sample was subjected to hematoxylin and eosin (H&E) staining. Stained sections were subjected to high-resolution scanning (Olympus VS120 Scanner) and the scans were uploaded for viewing on the web-based HALO® image hosting service. Immune cell aggregates, mature TLSs, and other areas of interest were electronically annotated and reviewed for accuracy by a trained pathologist (Minqi Xu).

An unstained section from each of the samples was stained via automated multiplex IF staining at the Molecular and Cellular Immunology Core facility (Deeley Research Centre; Vancouver, British Columbia, Canada). Samples were stained with fluorophore-conjugated primary antibodies against cell surface proteins to identify B cells, T cells, dendritic cells and high endothelial venules (**Suppl. Table S4**). Stained sections were scanned using the Vectra multispectral imaging system and viewed using PhenoChart 1.1.0 Software (Akoya BioSciences®; Marlborough, Massachusetts, USA). Aggregates/TLSs were classified into primary (immature) or secondary (mature) follicle as previously reported.[18]

4.3 Digital spatial profiling of NMIBC tumors using NanoString's GeoMx platform

We employed NanoString's GeoMx® DSP technology to spatially characterize the protein expression profiles in TLSs and epithelial regions within a subset of tumors from a subset of NMIBC 6 responders and 6 non-responders. This unique, high-throughput multiplexed technique uses indexing oligonucleotides to quantify the spatially resolved abundance of protein or RNA from FFPE tissue sections. Unstained fresh-cut 5 µm sections from the selected samples were processed on the NanoString GeoMx DSP platform at the Imaging Centre (University of Minnesota, USA). Slide processing was performed as per the manufacturer's instructions using DNA stain (SYTO 13), pan-Cytokeratin (epithelium), CD45 (immune cells) and CD20 (B cells) antibodies to guide selection of regions of interest. The abundance and localization of 49 immune proteins of interest (Immune Cell Profiling Core, plus the Immuno-Oncology, Drug Target Module, Immune Activation Status Module, and the Immune Cell Typing Module; see **Suppl. Table S2**) was measured. Quality control was performed as per the manufacturer's instructions and External RNA Controls Consortium in DSP suite (Ncounter® platform) prior to further analysis. Details of the DSP methodology and analysis are provided in the Supplementary data.

4.4. *In vivo* studies

Animal models

All murine experiments were in accordance with the guidelines provided by Queen's University Animal Care Committee and approved in an animal research protocol. The B6.Cg-Tg(Sry)2Ei Srydl1Rlb/ArnoJ mice were kindly provided by Dr. Manu Rangachari (University of Laval) and also purchased from the Jackson laboratory (stock number 010905, RRID:SCR_002187). Breeding of the FCG mice was conducted at the Queen's animal care facility to derive the four genotypes (gonadally female mice and male mice with XX and XY chromosomal complement each). The FCG transgenic mouse model (on a C57BL/6 background) allows for the generation of sex-reversed XX males and XY females by breeding mice with a loss-of-function mutation in the Y chromosome-linked

testes-determining Sry gene with transgenic mice carrying an Sry rescue transgene on an autosome. (**Fig. 4A**).[70] This model permits determination of independent effects of gonadal and sex chromosome-specific features on bladder cancer progression associated immunologic profiles. Mice were aged for 12 months at the facility. Wild type C57BL/6 male and female mice (3 months and 12 months old) were purchased from Charles River Laboratory (Montreal, QC, Canada). All mice were fed sterilized conventional diet and water and maintained under specific pathogen-free environment.

4.5 BBN carcinogen exposure and depletion of B cells

Female (3 months and 12 months old), male (12 months old) C57BL/6 mice and FCG mice (12 months old) were administered 0.05% BBN (Cat# B0938, TCI America, OR, USA); TCI America) *ad libitum* in drinking water (protected from light) once a week for 7-12 weeks as previously described.[23] Our previous findings have demonstrated the formation of lymphocyte aggregates, within the lamina propria of bladder, initiating at week 4 post first BBN administration.[23] To determine the influence of B cells on disease progression, we initiated B cell depletion starting week 3 post BBN exposure. Briefly, a cocktail of monoclonal antibodies (**Suppl. Table S3**) at 150 µg/mouse: rat anti-mouse CD19, rat anti-mouse B220 and mouse anti-mouse CD22 was injected via intraperitoneal (I.P) injection, as described previously.[71] After 48 hours, mice were injected with mouse anti-rat κ secondary antibody at 150 µg/mouse. To maintain the depletion of B cells *in vivo,* mice were injected with anti-CD20 antibody. B cell depletion cocktail injections were repeated 3 times every 10 days to ensure the complete depletion of systemic B cells, further confirmed with flow cytometry results post last injection.

To determine the effect of B cell depletion on response to BCG in BBN exposed mice, depletion protocol was initiated 1 week prior to 1st BCG instillation (section 4.6) followed by weekly anti-CD20 antibody injections for 3 weeks during BCG treatment. Isotype controls for each antibody (**Suppl. Table S3**) mentioned above was used as a control.

4.6 Intravesical BCG in BBN exposed mice

Lyophilized Tice strain of BCG (Merck, Canada) was obtained from the pharmacy at KHSC. Each 50 mg vial contained 1 to 8 x 10^8 colony forming unit (CFU) of BCG, as tested by the manufacturer. BCG was resuspended in sterile saline for all experiments. At 7 weeks post BBN exposure, mice were subjected to intravesical treatment with 3 weekly instillations of BCG (1mg/mouse in 50 µl) or saline. BCG was delivered via transurethral catheterization with a 24-gauge catheter (3/4", Cat# 4053, Jelco, Minneapolis, USA) for female mice and PE-10 tubing in male mice (procedure video) under isofluorane anaesthesia. Urethral VASCU-STATT Midi clamps (Cat# 1001-501, Scanlan, Canada) were placed to hold BCG within the bladder for 1 hour. Whole bladders were collected from all treatment groups post 1st (8 weeks post BBN exposure) and 3rd BCG (10 weeks post BBN exposure) instillation, post 1st anti-CD20 treatment after 1st BCG instillation (8 weeks post BBN exposure) and post 3rd anti-CD20 treatment after 3rd BCG (10 weeks post BBN exposure) instillation (**Fig. 3A**) and fixed in 4% paraformaldehyde for histopathological evaluation and spatial immune profiling via multiplex IF. Single cell suspensions from bone marrow and spleen were subjected to profiling using multispectral flow cytometry. Blood was collected from the submandibular vein for plasma cytokine profiling using multiplex cytokine analysis.

4.7 Local and Systemic immune profiling using multispectral flow cytometry

Whole bladders collected from all treatment groups, at treatment time points as indicated (section 4.6), were sagittaly cut into two halves and paraffin-embedded for H&E staining at the QLMP y as described in section 4.2. The urothelial changes in mice were classified as follows: reactive atypia, dysplasia, carcinoma *in situ* (CIS), early invasion and invasion. Five µm unstained FFPE sections were subjected to spatial immune profiling using multiplex IF staining to analyze infiltration patterns of selected immune markers using panel of antibodies to identify CD11b+ myeloid cells, CD3+ total T cells, CD8+ cytotoxic T cells, Pax5+ B cells, PD-L1+ immune checkpoint (Suppl. Table S1) IF staining was performed at the Molecular and Cellular Immunology Core (MCIC) facility, BC Cancer Agency as per previously reported methods[13,23]. Multiplex IF stained images were acquired using the Vectra 3

multichannel imaging system. Images were then imported to Phenochart (11.0, Akoya Biosciences) and Inform Viewer (2.5.0, Akoya Biosciences) software for annotation followed by capturing at high magnification. The Inform Viewer was used to visualize a detailed composite image of each section with the flexibility of spectral separation of all the fluorophores from each panel.

Single cell suspensions from spleens harvested were prepared by mechanical dissociation. Bone marrow was aspirated with RPMI-1640 media (Wisent Bioproducts, ON, Canada) using a 26-gauge needle and passing it through a 40 µm cell strainer followed by red blood cell (RBC) lysis. Details of further processing and multiparametric flow cytometry (Cytoflex-S; Beckman, USA) are provided in the Supplementary methods section.

4.8 Plasma cytokine profiling

Mice from each treatment group (n = 4-5 mice per group) were subjected to blood collection from the submandibular (facial) vein. Separated plasma was aliquoted as per the requirements for multiplex cytokine analysis and stored at -80°C until further profiling. Plasma was diluted using PBS (1:1) and subjected to multiplex cytokine analysis using commercially available 32-Plex Mouse Cytokine Discovery Array (MD-31; Eve Technologies, AB, Canada).

4.9 Statistical Analysis

Statistical analysis was performed using GraphPad Prism 9.0 (GraphPad, USA). Results are expressed as mean ± SD. Three or more groups were with one independent variable were analysed using one-way ANOVA with Tukey's post hoc test. Three or more groups with two or more independent variable were analysed using two-way ANOVA with Tukey's multiple comparison test. Statistical significance is indicated by *$p<0.05$, **$p<0.01$, ***$p<0.001$, ****$p<0.001$.

Author contributions and acknowledgements

MK conceptualized and designed the study. PY, SR, SC, GC and MK performed experiments included in this study, analyzed data and contributed to manuscript writing and reviewing. IE helped with BBN experiments. KS and JH analyzed the NanoString GeoMx DSP data. DJ helped with chart review and identification of BCG responders and non-responders. MX helped with reviewing histopathogical features and retrieving the archival tumor tissue specimens. DRS and DMB helped with clinical classifications of BCG treated patient specimens and reviewed the manuscript. This study was supported by research operating grants from Bladder Cancer Canada, Cancer Research Society, Ontario Ministry of Research Innovation and Science: Early Researcher Award and Canada Foundation for Innovation, to MK. We thank Shakeel Virk at the QLMP for his assistance with imaging and Halo software and Katy Milne at BC Cancer's Molecular and Cellular Immunology Core (MCIC) for immunofluorescence staining of TMAs. Dr. Patricia Lima at the Queen's Cardiopulmonary Unit helped with optimization of ABC panel and confocal microscopy-based imaging of multiplex IF stained whole bladder sections. We thank Dr. Andrew Winterborn and the staff at the Queen's animal care facility for all the support with animal studies.

References

1 Lobo, N. *et al.* Epidemiology, Screening, and Prevention of Bladder Cancer. *Eur Urol Oncol* **5**, 628-639 (2022). https://doi.org:10.1016/j.euo.2022.10.003

2 Saginala, K. *et al.* Epidemiology of Bladder Cancer. *Med Sci (Basel)* **8** (2020). https://doi.org:10.3390/medsci8010015

3 Richters, A., Leliveld, A. M., Goossens-Laan, C. A., Aben, K. K. H. & Ozdemir, B. C. Sex differences in treatment patterns for non-advanced muscle-invasive bladder cancer: a descriptive analysis of 3484 patients of the Netherlands Cancer Registry. *World J Urol* **40**, 2275-2281 (2022). https://doi.org:10.1007/s00345-022-04080-6

4 Viswambaram, P. & Hayne, D. Gender discrepancies in bladder cancer: potential explanations. *Expert Rev Anticancer Ther* **20**, 841-849 (2020). https://doi.org:10.1080/14737140.2020.1813029

5 Gul, Z. G., Liaw, C. W. & Mehrazin, R. Gender Differences in Incidence, Diagnosis, Treatments, and Outcomes in Clinically Localized Bladder and Renal Cancer. *Urology* **151**, 176-181 (2021). https://doi.org:10.1016/j.urology.2020.05.067

6 Marks, P. *et al.* Female with bladder cancer: what and why is there a difference? *Transl Androl Urol* **5**, 668-682 (2016). https://doi.org:10.21037/tau.2016.03.22

7 Bree, K. K. *et al.* All High-Grade Ta Tumors Should Be Classified as High Risk: Bacillus Calmette-Guerin Response in High-Grade Ta Tumors. *J Urol* **208**, 284-291 (2022). https://doi.org:10.1097/JU.0000000000002678

8 Babjuk, M. *et al.* European Association of Urology Guidelines on Non-muscle-invasive Bladder Cancer (Ta, T1, and Carcinoma in Situ). *Eur Urol* **81**, 75-94 (2022). https://doi.org:10.1016/j.eururo.2021.08.010

9 Roumiguie, M. *et al.* International Bladder Cancer Group Consensus Statement on Clinical Trial Design for Patients with Bacillus Calmette-Guerin-exposed High-risk Non-muscle-invasive Bladder Cancer. *Eur Urol* (2021). https://doi.org:10.1016/j.eururo.2021.12.005

10 Lobo, N. *et al.* Updated European Association of Urology (EAU) Prognostic Factor Risk Groups Overestimate the Risk of Progression in Patients with Non-muscle-invasive Bladder Cancer Treated with Bacillus Calmette-Guerin. *Eur Urol Oncol* (2021). https://doi.org:10.1016/j.euo.2021.11.006

11 Packiam, V. T., Richards, J., Schmautz, M., Heidenreich, A. & Boorjian, S. A. The current landscape of salvage therapies for patients with bacillus Calmette-Guerin unresponsive nonmuscle invasive bladder cancer. *Curr Opin Urol* **31**, 178-187 (2021). https://doi.org:10.1097/MOU.0000000000000863

12 Flaig, T. W. *et al.* NCCN Guidelines(R) Insights: Bladder Cancer, Version 2.2022. *J Natl Compr Canc Netw* **20**, 866-878 (2022). https://doi.org:10.6004/jnccn.2022.0041

13 Chenard, S. *et al.* Sexual Dimorphism in Outcomes of Non-muscle-invasive Bladder Cancer: A Role of CD163+ Macrophages, B cells, and PD-L1 Immune Checkpoint. *Eur Urol Open Sci* **29**, 50-58 (2021). https://doi.org:10.1016/j.euros.2021.05.002

14 Salome, B. *et al.* NKG2A and HLA-E define an alternative immune checkpoint axis in bladder cancer. *Cancer Cell* **40**, 1027-1043 e1029 (2022). https://doi.org:10.1016/j.ccell.2022.08.005

15 Strandgaard, T. *et al.* Elevated T-cell Exhaustion and Urinary Tumor DNA Levels Are Associated with Bacillus Calmette-Guerin Failure in Patients with Non-muscle-invasive Bladder Cancer. *Eur Urol* **82**, 646-656 (2022). https://doi.org:10.1016/j.eururo.2022.09.008

16 Kates, M. *et al.* Adaptive Immune Resistance to Intravesical BCG in Non-Muscle Invasive Bladder Cancer: Implications for Prospective BCG-Unresponsive Trials. *Clin Cancer Res* **26**, 882-891 (2020). https://doi.org:10.1158/1078-0432.CCR-19-1920

17 Booth, J. S. & Toapanta, F. R. B and T Cell Immunity in Tissues and Across the Ages. *Vaccines (Basel)* **9** (2021). https://doi.org:10.3390/vaccines9010024

18 Schumacher, T. N. & Thommen, D. S. Tertiary lymphoid structures in cancer. *Science* **375**, eabf9419 (2022). https://doi.org:10.1126/science.abf9419
19 Tam, A. *et al.* Sex differences in lymphoid follicles in COPD airways. *Respir Res* **21**, 46 (2020). https://doi.org:10.1186/s12931-020-1311-8
20 Lu, K. *et al.* Identification of novel biomarkers in Hunner's interstitial cystitis using the CIBERSORT, an algorithm based on machine learning. *BMC Urol* **21**, 109 (2021). https://doi.org:10.1186/s12894-021-00875-8
21 Akiyama, Y. *et al.* Autoimmunity to urothelial antigen causes bladder inflammation, pelvic pain, and voiding dysfunction: a novel animal model for Hunner-type interstitial cystitis. *Am J Physiol Renal Physiol* **320**, F174-F182 (2021). https://doi.org:10.1152/ajprenal.00290.2020
22 Ligon, M. M. *et al.* Single cell and tissue-transcriptomic analysis of murine bladders reveals age- and TNFalpha-dependent but microbiota-independent tertiary lymphoid tissue formation. *Mucosal Immunol* (2020). https://doi.org:10.1038/s41385-020-0290-x
23 Hamade, A. *et al.* Sex differences in the aging murine urinary bladder and influence on the tumor immune microenvironment of a carcinogen-induced model of bladder cancer. *Biol Sex Differ* **13**, 19 (2022). https://doi.org:10.1186/s13293-022-00428-0
24 Koti, M. *et al.* Tertiary Lymphoid Structures Associate with Tumour Stage in Urothelial Bladder Cancer. *Bladder Cancer* **3**, 259-267 (2017). https://doi.org:10.3233/BLC-170120
25 Marquez, E. J. *et al.* Sexual-dimorphism in human immune system aging. *Nat Commun* **11**, 751 (2020). https://doi.org:10.1038/s41467-020-14396-9
26 Phalke, S. *et al.* Molecular mechanisms controlling age-associated B cells in autoimmunity. *Immunol Rev* (2022). https://doi.org:10.1111/imr.13068
27 Moyron-Quiroz, J. E. *et al.* Role of inducible bronchus associated lymphoid tissue (iBALT) in respiratory immunity. *Nat Med* **10**, 927-934 (2004). https://doi.org:10.1038/nm1091
28 Rangel-Moreno, J. *et al.* Omental milky spots develop in the absence of lymphoid tissue-inducer cells and support B and T cell responses to peritoneal antigens. *Immunity* **30**, 731-743 (2009). https://doi.org:10.1016/j.immuni.2009.03.014
29 Robson, K. J. & Kitching, A. R. Tertiary lymphoid tissue in kidneys: understanding local immunity and inflammation. *Kidney Int* **98**, 280-283 (2020). https://doi.org:10.1016/j.kint.2020.04.026
30 Rubtsov, A. V. *et al.* Toll-like receptor 7 (TLR7)-driven accumulation of a novel CD11c(+) B-cell population is important for the development of autoimmunity. *Blood* **118**, 1305-1315 (2011). https://doi.org:10.1182/blood-2011-01-331462
31 Sachinidis, A., Xanthopoulos, K. & Garyfallos, A. Age-Associated B Cells (ABCs) in the Prognosis, Diagnosis and Therapy of Systemic Lupus Erythematosus (SLE). *Mediterr J Rheumatol* **31**, 311-318 (2020). https://doi.org:10.31138/mjr.31.3.311
32 Hao, Y., O'Neill, P., Naradikian, M. S., Scholz, J. L. & Cancro, M. P. A B-cell subset uniquely responsive to innate stimuli accumulates in aged mice. *Blood* **118**, 1294-1304 (2011). https://doi.org:10.1182/blood-2011-01-330530
33 Mouat, I. C. & Horwitz, M. S. Age-associated B cells in viral infection. *PLoS Pathog* **18**, e1010297 (2022). https://doi.org:10.1371/journal.ppat.1010297
34 Cancro, M. P. Age-Associated B Cells. *Annu Rev Immunol* **38**, 315-340 (2020). https://doi.org:10.1146/annurev-immunol-092419-031130
35 Ratliff, M., Alter, S., Frasca, D., Blomberg, B. B. & Riley, R. L. In senescence, age-associated B cells secrete TNFalpha and inhibit survival of B-cell precursors. *Aging Cell* **12**, 303-311 (2013). https://doi.org:10.1111/acel.12055
36 Riley, R. L., Khomtchouk, K. & Blomberg, B. B. Age-associated B cells (ABC) inhibit B lymphopoiesis and alter antibody repertoires in old age. *Cell Immunol* **321**, 61-67 (2017). https://doi.org:10.1016/j.cellimm.2017.04.008

37 Zhang, W. *et al.* Excessive CD11c(+)Tbet(+) B cells promote aberrant TFH differentiation and affinity-based germinal center selection in lupus. *Proc Natl Acad Sci U S A* **116**, 18550-18560 (2019). https://doi.org:10.1073/pnas.1901340116

38 Rakhmanov, M. *et al.* Circulating CD21low B cells in common variable immunodeficiency resemble tissue homing, innate-like B cells. *Proc Natl Acad Sci U S A* **106**, 13451-13456 (2009). https://doi.org:10.1073/pnas.0901984106

39 Mouat, I. C., Goldberg, E. & Horwitz, M. S. Age-associated B cells in autoimmune diseases. *Cell Mol Life Sci* **79**, 402 (2022). https://doi.org:10.1007/s00018-022-04433-9

40 Guerrier, T. *et al.* TLR9 expressed on plasma membrane acts as a negative regulator of human B cell response. *J Autoimmun* **51**, 23-29 (2014). https://doi.org:10.1016/j.jaut.2014.02.005

41 Cornelie, S. *et al.* Direct evidence that toll-like receptor 9 (TLR9) functionally binds plasmid DNA by specific cytosine-phosphate-guanine motif recognition. *J Biol Chem* **279**, 15124-15129 (2004). https://doi.org:10.1074/jbc.M313406200

42 Antonelli, A. C., Binyamin, A., Hohl, T. M., Glickman, M. S. & Redelman-Sidi, G. Bacterial immunotherapy for cancer induces CD4-dependent tumor-specific immunity through tumor-intrinsic interferon-γ signaling. *Proc Natl Acad Sci U S A* **117**, 18627-18637 (2020). https://doi.org:10.1073/pnas.2004421117

43 Kaufmann, E. *et al.* BCG Educates Hematopoietic Stem Cells to Generate Protective Innate Immunity against Tuberculosis. *Cell* **172**, 176-190 e119 (2018). https://doi.org:10.1016/j.cell.2017.12.031

44 Bafica, A. *et al.* TLR9 regulates Th1 responses and cooperates with TLR2 in mediating optimal resistance to Mycobacterium tuberculosis. *J Exp Med* **202**, 1715-1724 (2005). https://doi.org:10.1084/jem.20051782

45 Van Dis, E. *et al.* STING-Activating Adjuvants Elicit a Th17 Immune Response and Protect against Mycobacterium tuberculosis Infection. *Cell Rep* **23**, 1435-1447 (2018). https://doi.org:10.1016/j.celrep.2018.04.003

46 von Meyenn, F. *et al.* Toll-like receptor 9 contributes to recognition of Mycobacterium bovis Bacillus Calmette-Guerin by Flt3-ligand generated dendritic cells. *Immunobiology* **211**, 557-565 (2006). https://doi.org:10.1016/j.imbio.2006.05.004

47 Yu, B. *et al.* B cell-specific XIST complex enforces X-inactivation and restrains atypical B cells. *Cell* **184**, 1790-1803 e1717 (2021). https://doi.org:10.1016/j.cell.2021.02.015

48 Joudi, F. N., Smith, B. J., O'Donnell, M. A. & Konety, B. R. The Impact of Age on the Response of Patients With Superficial Bladder Cancer to Intravesical Immunotherapy. *Journal of Urology* **175**, 1634-1640 (2006). https://doi.org:10.1016/s0022-5347(05)00973-0

49 Rodriguez, A. B. & Engelhard, V. H. Insights into Tumor-Associated Tertiary Lymphoid Structures: Novel Targets for Antitumor Immunity and Cancer Immunotherapy. *Cancer Immunol Res* **8**, 1338-1345 (2020). https://doi.org:10.1158/2326-6066.CIR-20-0432

50 Meylan, M. *et al.* Tertiary lymphoid structures generate and propagate anti-tumor antibody-producing plasma cells in renal cell cancer. *Immunity* (2022). https://doi.org:10.1016/j.immuni.2022.02.001

51 Goswami, S. *et al.* ARID1A mutation plus CXCL13 expression act as combinatorial biomarkers to predict responses to immune checkpoint therapy in mUCC. *Sci Transl Med* **12** (2020). https://doi.org:10.1126/scitranslmed.abc4220

52 Kroeger, D. R., Milne, K. & Nelson, B. H. Tumor-Infiltrating Plasma Cells Are Associated with Tertiary Lymphoid Structures, Cytolytic T-Cell Responses, and Superior Prognosis in Ovarian Cancer. *Clin Cancer Res* **22**, 3005-3015 (2016). https://doi.org:10.1158/1078-0432.CCR-15-2762

53 Pfannstiel, C. *et al.* The Tumor Immune Microenvironment Drives a Prognostic Relevance That Correlates with Bladder Cancer Subtypes. *Cancer Immunol Res* **7**, 923-938 (2019). https://doi.org:10.1158/2326-6066.CIR-18-0758
54 Groeneveld, C. S. *et al.* Tertiary lymphoid structures marker CXCL13 is associated with better survival for patients with advanced-stage bladder cancer treated with immunotherapy. *Eur J Cancer* **148**, 181-189 (2021). https://doi.org:10.1016/j.ejca.2021.01.036
55 Sakimura, C. *et al.* B cells in tertiary lymphoid structures are associated with favorable prognosis in gastric cancer. *J Surg Res* **215**, 74-82 (2017). https://doi.org:10.1016/j.jss.2017.03.033
56 Tang, J. *et al.* B Cells and Tertiary Lymphoid Structures Influence Survival in Lung Cancer Patients with Resectable Tumors. *Cancers (Basel)* **12** (2020). https://doi.org:10.3390/cancers12092644
57 Finkin, S. *et al.* Ectopic lymphoid structures function as microniches for tumor progenitor cells in hepatocellular carcinoma. *Nat Immunol* **16**, 1235-1244 (2015). https://doi.org:10.1038/ni.3290
58 Figenschau, S. L., Fismen, S., Fenton, K. A., Fenton, C. & Mortensen, E. S. Tertiary lymphoid structures are associated with higher tumor grade in primary operable breast cancer patients. *BMC Cancer* **15**, 101 (2015). https://doi.org:10.1186/s12885-015-1116-1
59 Bento, D. C. *et al.* High endothelial venules are rare in colorectal cancers but accumulate in extra-tumoral areas with disease progression. *Oncoimmunology* **4**, e974374 (2015). https://doi.org:10.4161/2162402X.2014.974374
60 Jallad, S., Goubet, S., Symes, A., Larner, T. & Thomas, P. Prognostic value of inflammation or granuloma after intravesival BCG in non-muscle-invasive bladder cancer. *BJU Int* **113**, E22-27 (2014). https://doi.org:10.1111/bju.12334
61 Pipi, E. *et al.* Tertiary Lymphoid Structures: Autoimmunity Goes Local. *Frontiers in Immunology* **9** (2018). https://doi.org:10.3389/fimmu.2018.01952
62 Zlotta, A. R. *et al.* Humoral response against heat shock proteins and other mycobacterial antigens after intravesical treatment with bacille Calmette-Guerin (BCG) in patients with superficial bladder cancer. *Clin Exp Immunol* **109**, 157-165 (1997). https://doi.org:10.1046/j.1365-2249.1997.4141313.x
63 Shlesinger, D. *et al.* Single-cell immune repertoire sequencing of B and T cells in murine models of infection and autoimmunity. *Genes Immun* **23**, 183-195 (2022). https://doi.org:10.1038/s41435-022-00180-w
64 Hinrichs, C. S. *et al.* IL-2 and IL-21 confer opposing differentiation programs to CD8+ T cells for adoptive immunotherapy. *Blood* **111**, 5326-5333 (2008). https://doi.org:10.1182/blood-2007-09-113050
65 Welten, S. P. M. *et al.* Tcf1(+) cells are required to maintain the inflationary T cell pool upon MCMV infection. *Nat Commun* **11**, 2295 (2020). https://doi.org:10.1038/s41467-020-16219-3
66 Moir, S. *et al.* Evidence for HIV-associated B cell exhaustion in a dysfunctional memory B cell compartment in HIV-infected viremic individuals. *J Exp Med* **205**, 1797-1805 (2008). https://doi.org:10.1084/jem.20072683
67 Knox, J. J., Myles, A. & Cancro, M. P. T-bet(+) memory B cells: Generation, function, and fate. *Immunol Rev* **288**, 149-160 (2019). https://doi.org:10.1111/imr.12736
68 Marquart, H. V. *et al.* Complement receptor expression and activation of the complement cascade on B lymphocytes from patients with systemic lupus erythematosus (SLE). *Clin Exp Immunol* **101**, 60-65 (1995). https://doi.org:10.1111/j.1365-2249.1995.tb02277.x
69 Krocova, Z. *et al.* The role of B cells in an early immune response to Mycobacterium bovis. *Microb Pathog* **140**, 103937 (2020). https://doi.org:10.1016/j.micpath.2019.103937
70 Itoh, Y. *et al.* Four core genotypes mouse model: localization of the Sry transgene and bioassay for testicular hormone levels. *BMC Res Notes* **8**, 69 (2015). https://doi.org:10.1186/s13104-015-0986-2

71 Keren, Z. *et al.* B-cell depletion reactivates B lymphopoiesis in the BM and rejuvenates the B lineage in aging. *Blood* **117**, 3104-3112 (2011). https://doi.org:10.1182/blood-2010-09-307983